Perturbations of GPS signals by the ionospheric irregularities generated due to HF-heating at triple of electron gyrofrequency

Gennady Milikh,[1] Alex Gurevich,[2] Kiril Zybin,[2] and Jim Secan[3]

Received 30 July 2008; revised 2 October 2008; accepted 6 October 2008; published 19 November 2008.

[1] The objective of this letter is to present the first experimental evidence of perturbations of GPS signals by the electron density irregularities caused by the HF-heating of the F_2 region of the ionosphere. The experiments were conducted using the HAARP heater having the radiating frequency f which matches 3 f_B, i.e., triple the local electron gyro frequency. Such frequency is expected to generate super small irregularities of the electron density which can scatter GPS signals. It was found that the differential phase of the probe GPS signals changed abruptly in about 10 s after the start of the HF-heating, and then oscillated with the heating period 20 s. The oscillations lasted for 4–5 minutes and then disappeared, presumably when the resonance condition $f = 3\ f_B$ was not satisfied, although the HF-heating continued. The phase oscillations indicate the presence of small scale irregularities of the electron density caused by the HF-heating at the frequency matching 3 f_B.
Citation: Milikh, G., A. Gurevich, K. Zybin, and J. Secan (2008), Perturbations of GPS signals by the ionospheric irregularities generated due to HF-heating at triple of electron gyrofrequency, *Geophys. Res. Lett.*, *35*, L22102, doi:10.1029/2008GL035527.

1. Introduction

[2] Generation of artificial field-aligned irregularities of electron density due to the ionospheric heating by powerful radio waves of O-mode was first discovered at Platteville [*Thome and Blood*, 1974; *Fialer*, 1974]. Later this effect was confirmed by experiments conducted at other HF-heating facilities [*Hansen et al.*, 1992; *Kelley et al.*, 1995; *Bakhmet'eva et al.*, 1997; *Dhillon and Robinson*, 2005]. It was found that the wavelength spectrum of the artificial irregularities was in the range from tens of meters to kilometers. On a few occasions striations of a size slightly less than 10 m were observed [*Dhillon and Robinson*, 2005]. Different mechanisms for the generation of field-aligned irregularities of electron density due to HF-heating were suggested [*Gurevich*, 2007].

[3] In fact, ponderomotive parametric instability develops during the first 5–20 ms of the heating. Thermal (resonant) parametric instability develops over a few seconds [*Vaskov and Gurevich*, 1976; *Mjolhus*, 1993; *Gurevich et al.*, 1995]. It generates upper hybrid plasma turbulence and produces small scale ionospheric irregularities having transversal scale sizes of 30–50 m. Self-focusing instability develops over 10–30 s, and generates middle scale irregularities of transverse scale size 0.1–1 km [*Gurevich et al.*, 1996; *Gondarenko et al.*, 2005]. Finally, magnification of the natural irregularities causes large scale irregularities having scale sizes larger than 1–2 km.

[4] A new mechanism for generation of super small scale field-aligned irregularities of the size of tens centimeters was recently suggested by *Gurevich and Zybin* [2006]. According to this model, the upper hybrid waves due to HF-heating at harmonics of the electron gyrofrequency can be trapped inside striations producing standing Bernstein waves. The latter waves have large amplitude, and thus produce the ponderomotive force which in turn pushes plasma away from the electric field peaks. As a result the plasma irregularities are created having the transverse scale size $\lambda/2$ where $\lambda \sim 10$–40 cm is the Bernstein wavelength, while the longitudinal scale size is of about 1 km. These field aligned irregularities were termed super small scale (SSS) irregularities. The best way to examine this phenomenon is by using diagnostics of UHF radio waves, in particular GPS signals.

[5] The objective of this letter is to present the first experimental evidence of strong perturbations of GPS signals by the irregularities of the electron density caused by the HF-heating of the F_2 region of the ionosphere. The experiments were conducted using the HAARP IRI (Ionospheric Research Instrument) with the radiating frequency close to the triple electron gyro frequency, 3 f_B. The super small scale irregularities which scatter GPS signals can play an important role in many applications such as in the effects of powerful broadcasting facilities on UHF propagation.

[6] The letter is organized as following: Section 2 describes layout of the experiments. Section 3 discusses the data collection and processing technique. Section 4 presents discussion and conclusions.

2. Layout of the Ionospheric Heating Experiments

[7] Six observations were conducted during the 2008 Winter HARP campaign: 02/22, 02/23, 02/24 (twice), 02/25, and 02/26. Each of these days the HF-heating lasted for 20 minutes around 19 UT, with the exception of 02/24, in which case two observations were conducted starting at 18:28 and 19:13. We used the heating frequency $f = 3\ f_B$ considering that f_B depends upon the altitude. In fact, f_B drops from 4.24 MHz to 4.05 MHz when the altitude increases from 250 km to 350 km. The exact choice of the heating frequency changed from day to day depending upon the local ionospheric conditions. Our main limitation

[1]Department of Astronomy, University of Maryland, College Park, Maryland, USA.
[2]P. N. Lebedev Institute, Russian Academy of Sciences, Moscow, Russia.
[3]Northwest Research Associates Inc., Tucson, Arizona, USA.

0094-8276/08/2008GL035527$05.00

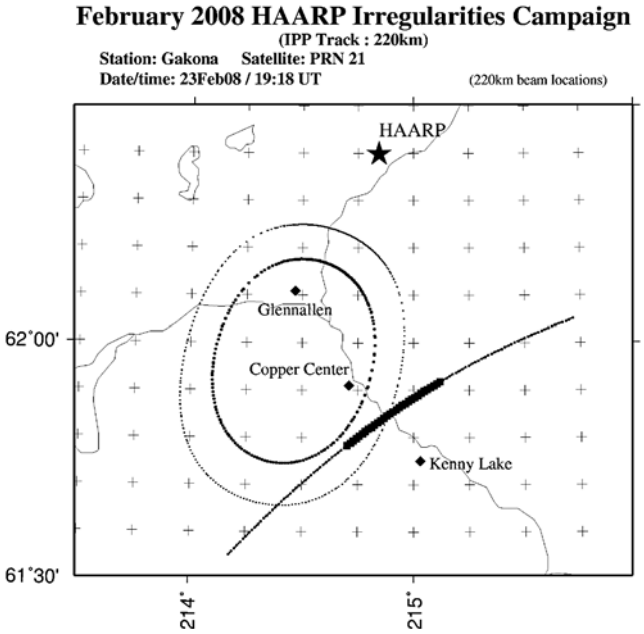

Figure 1. The track of the 220 km Ionospheric Penetration Point (IPP) for GPS PRN 21 during the experiment. The track begins at the lower-left side and moves across to the upper-left. The heavy section of the track indicates the IPP locations during the HF-heating. The oval-shaped regions demark the 3dB (inner oval) and 6dB (outer oval) contours of the heater beam, mapped to an altitude of 220 km. The heater facility location is indicated by a star labeled "HAARP".

was keeping the chosen heating frequency $f = 3\,f_B$ below the F_2-layer critical frequency ($f < f_0F_2$), otherwise the HF beam propagates through the F_2-layer with almost no absorption, and thus causes only minor effect in the ionosphere. Based on the above considerations we chose the following heating frequencies: 02/22/08 we used f = 4.04 MHz; 02/23/08 we used f = 4.3 MHz; 02/24/08 we used f = 4.1 MHz and 4.23 MHz during first and second heating periods respectively; 02/25/08 and 02/26/08 we used f = 4.3 MHz. In each of these experiments we kept the chosen frequency constant over the entire 20 minute operation. In all these cases, the on-site HAARP diagnostics indicated a smooth F-region layer, a negligible D/E region absorption and absence of an electrojet current.

[8] We used square pulses having pulse width of 10 seconds with 10 seconds between the pulses in O-mode, and with maximum effective radiated power (ERP). For the chosen frequencies the ERP was about 89 dBW, while the beam half-power width was about 14° in the North–South direction and 10° in the East–West direction. The beam was directed along the magnetic zenith corresponding to 14° at the HAARP location. During the last 5 minutes of the designated observational time, we switched to 0.2 s square pulse modulation in an attempt to check the rising time of the instability. The critical diagnostic instrument is a GPS receiver located at HAARP which detects the changes in phases of GPS signals passing through the HF-heated spot. Signals from two GPS satellites PRN 06 and PRN 21 were received at HAARP with the sampling rate 2.0 Hz. Particularly we used data from PRN 21 for the passes on 02/22, 02/23, 02/25 and 02/26 and from PRN 06 for the pass on 24 February.

3. Data Collection and Processing

[9] The data is obtained using a dual-frequency Ashtech Z-FX GPS receiver located at the HAARP facility. Geometry of the experiment is illustrated by Figure 1. Data acquisition and initial processing are done on a PC running the NorthWest Research Associates (NWRA) GPS Ionospheric Observing System (GIOS) software package. The raw data used in this analysis is the observed phases and group-delay on both the L1 (1575.42 MHz) and L2 (1227.60 MHz) frequencies at a cadence of two samples per second. The raw data is converted to estimates of the absolute Slant Total Electron Content (STEC) as follows:

[10] The L1 and L2 phase observations (ϕ_1 and ϕ_2) are converted to differential carrier phase (DCP) using

$$\Delta\phi = \phi_1 - \frac{f_1}{f_2}\phi_2 \ cycles \tag{1}$$

where f_1 and f_2 are the L1 and L2 frequencies, respectively. Since this is a relative measurement, the resulting DCP time series is adjusted by a constant offset so that the initial DCP value is zero.

[11] The DCP time series is checked for phase jumps (indicative of a phase "cycle slip" in the receiver) which are removed by resetting the offset used in the time series after the time of the jump. This additional offset is either the difference between the DCP values on either side of the jump if the time step between the two is less than one second, or to the difference between linear fits to the DCP series on either side of the jump if otherwise. This algorithm also checks for and removes outliers.

[12] The cleaned DCP values are then converted to relative STEC estimates ($\Delta N_{T\phi}$) using

$$\Delta N_{T\phi} = \frac{f_1}{K\left[1 - \left(f_1/f_2\right)^2\right]}\Delta\phi \ \text{TECU} \tag{2}$$

where 1 TECU = 1.0×10^{16} el/m^2. The constant K is given by

$$K = \frac{e^2}{8\pi^2 m_e c \varepsilon_0} = 1.34454 \times 10^{-7} \ \text{rad/TECU} \tag{3}$$

where e is the electron charge, m_e is the electron mass, c is the vacuum light speed, and ε_0 is the permittivity of free space.

[13] The group-delay observations on L1 and L2 are used to provide an estimate of the absolute STEC (including an instrument bias) using

$$N_{TG} = \frac{f_1^2}{K\left[1 - \left(f_1/f_2\right)^2\right]}(\tau_1 - \tau_2) \ \text{TECU} \tag{4}$$

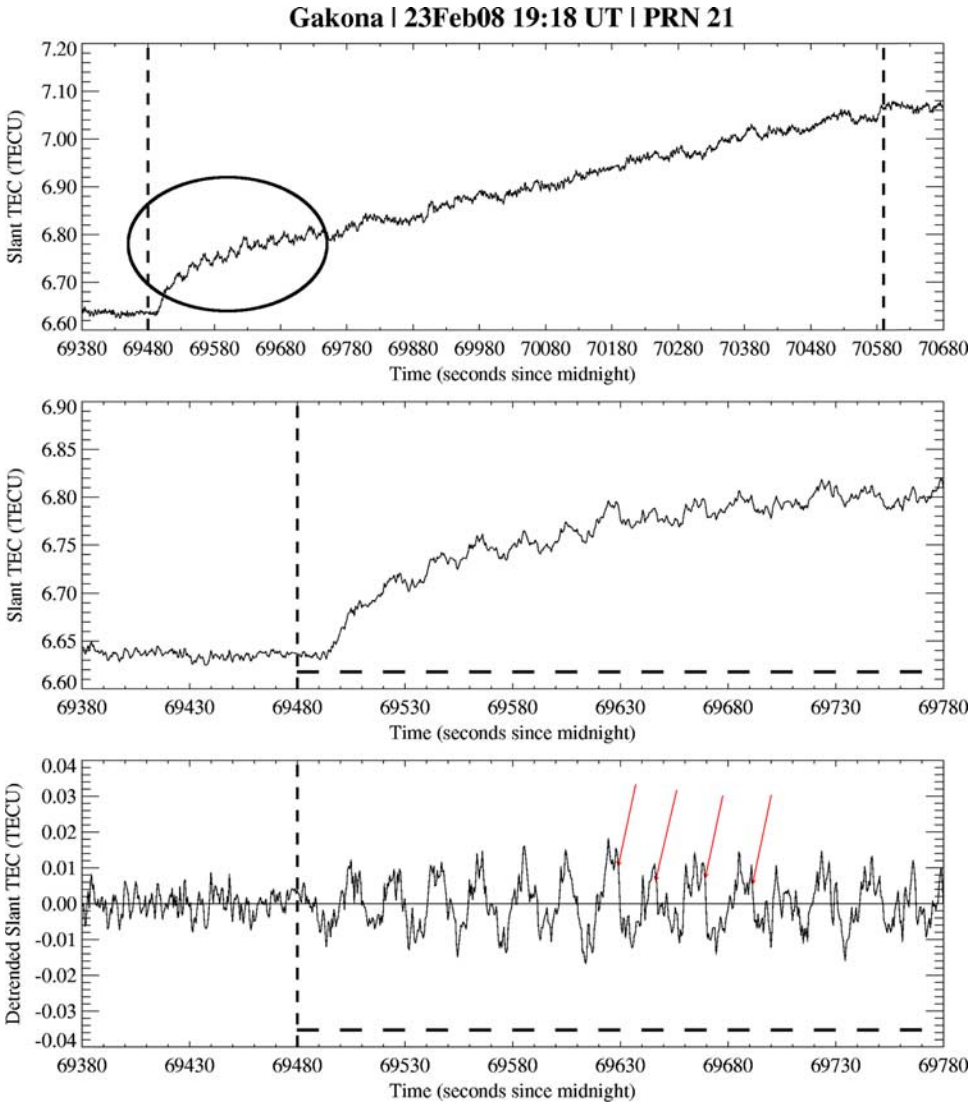

Figure 2. (top) Absolute STEC versus the observational time is revealed. The encircled area shows oscillations with 20 s period. (middle) The 5 minutes period of STEC oscillations is zoomed, while (bottom) the de-trended STEC during the same period is shown. The beginning and end of the HF-heating are marked by the vertical dashed lines. The black horizontal bars show the heating periods, each is 10 s long.

where τ_1 and τ_2 are the group-delays measured on the L1 and L2 frequencies (seconds). The N_{TG} STEC estimate provides a coarse estimate of the absolute STEC, and the $\Delta N_{T\phi}$ STEC estimate provides a precise estimate of relative STEC. The two can be combined using a method known as phase-averaging which uses the N_{TG} to provide a good estimate of the average STEC for the entire pass and the $\Delta N_{T\phi}$ to provide the variations relative to that base. This combined estimate of (biased) STEC will be denoted N_{TB}.

[14] The bias referred to earlier is due to unknown additional group-delay in both L1 and L2 in the satellite and in the receiver, which results in a biased estimate of the relative group-delay used in equation (4). As part of the routine processing of data collected by the HAARP GIOS system, estimates of these biases for each satellite are generated using the SCORE (Self-Calibration Of Range Errors) process [*Bishop et al.*, 1995]. This estimated bias for the satellite from which the observations were made is subtracted from N_{TB} to provide the final estimate of STEC, N_T.

[15] In order to more clearly observe the small-scale features that we expect to be generated by the interaction between the HAARP IRI beam and the ionosphere, the N_T time-series is detrended to remove ionospheric plasma-density structures with scale sizes larger than roughly 20 km by passing the time-series through a high-pass filter with a 0.025 Hz (40 second) 3-dB cut-off frequency. This filter is constructed from a six-pole Butterworth filter, and the time series is passed through the filter in both forward and reverse time direction to remove the offset incurred by a single pass through the filter. The output from the filter is a smoothed version of the original time series, with all fluctuations larger than the cut-off frequency removed. This "trend" time-series is then subtracted from the original time-series to produce the final detrended time series of STEC, denoted by ΔN_T. This filter has been used exten-

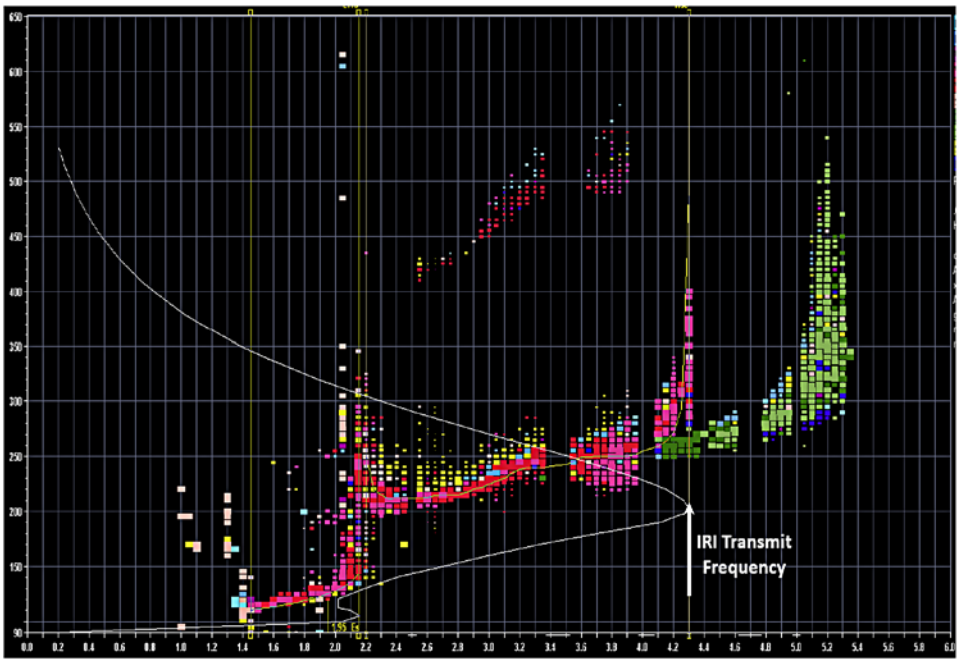

Figure 3. The ionogram taken at HAARP 02/23/08 at 19:20 UT by the digisonde. The points show virtual reflection heights versus frequency for four separate radio rays coming from different directions. The solid trace shows the extrapolated virtual reflection height. The ionogram reveals a smooth daytime F-layer, a moderate D/E region, and absence of the electrojet current.

sively in processing scintillation observations [*Fremouw et al.*, 1978].

[16] The complementary diagnostics include ionograms obtained with the help of the HAARP digisonde, diagnostics by the SuperDARN Kodiak radar, and observations of stimulated electromagnetic emission (SEE) made at the HAARP site. Kodiak radar diagnostics is used to obtain the spectrum of irregularities caused by the HF heating. The optical diagnostics although desirable is not applicable since the experiments were conducted during the local daytime. SEE observations could provide us with the test for matching the resonance conditions since the shape of the SEE spectrum changes when the resonance condition is met [*Gurevich*, 2007]. We use the ionograms taken each 5 minutes to select the proper heating frequencies, and to monitor the changes in the ionosphere and their effect on the excitation of small scale irregularities.

4. Discussion and Conclusions

[17] In four out of six observations we find that after the start of the heating the STEC of the probe GPS signals change abruptly in about 10 s, and then oscillate with the period of HF-heating, viz. 20 s. The oscillations last for 4–5 minutes and then disappear, presumably when the resonance condition is not satisfied, although the HF-heating continued. This is illustrated by Figure 2 obtained 02/23/08. Figure 2 (top) reveals the absolute STEC versus the observational time. Two vertical lines show the beginning and the end of the HF-heating. The encircled area shows oscillations with 20 s period. Figure 2 (middle) zooms the 5 minutes period when the STEC oscillations were detected, while Figure 2 (bottom) shows de-trended STEC during the same period.

[18] Note that our attempt to use 0.2 s square pulses modulation to check the rise time of the instability, which is estimated as 0.1 s, is unsuccessful. The main reason for this shortcoming is low sampling rate of the receiver, 2.0 Hz.

[19] HAARP digisonde developed by the University of Massachusetts, Lowell shows virtual reflection heights as function of frequency for four separate radio rays coming from South–East, South–West and North–East, North–West directions. Since the heating beam in our experiments is directed along the local magnetic zenith, i.e., is southward, we focus on the South–East/West rays (shown in red online). Figure 3 reveals the ionogram obtained 02/23/08 at 19:20 UT. Here the arrow shows the radiated frequency of the IRI. It shows that the heating frequency ($f = 3\,f_B$) is close to f_0F_2 for the SSE ray, and since the heating frequency has matched the F_2-layer critical frequency it is efficient in generating the ionospheric turbulence.

[20] The next ionogram taken in 10 minutes at 19:30 UT of February 23 is shown in Figure 4. It reveals that at this time F_2 peak moves downward leading to a mismatch between the heating frequency and f_0F_2. In fact, when the heating frequency becomes higher than f_0F_2 the ionospheric turbulence disappears.

[21] The Kodiak radar data shows that the backscatter power of the radar beam directed toward HAARP is reduced by 3–5 dB when triple the electron gyro frequency is reached. It indicates that the observed perturbations of GPS signals correlate with the change in reflecting properties of the ionospheric plasma.

[22] The SEE data shows that during all heating intervals with the frequency close to the triple gyro frequency, the downshifted maximum (DSM), which is the second maximum in the SEE spectrum downshifted by 10–15 kHz, is

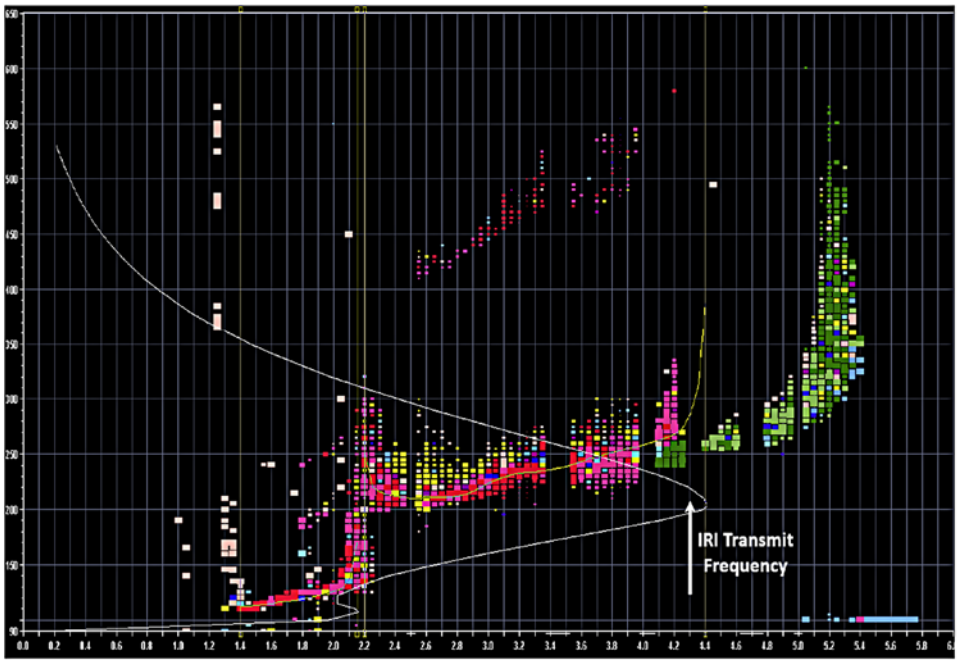

Figure 4. The ionogram taken at HAARP ten minutes later the same day, under similar ionospheric conditions.

suppressed. This is consistent with a reduction in the striations amplitude. The difference between the SEE peak which corresponds to the reflected heating wave and DSM is smaller than −30 dB while in the regular observations it is about −(15–20) dB [*Stubbe et al.*, 1994]. At the same time, the upshifted maximum which appears at the heating by the fourth gyro harmonic [*Stubbe et al.*, 1994] is not observed. The obtained SEE spectrum cannot distinguish the time intervals when the SSS irregularities where detected, which will be a subject of future studies.

[23] The smallest scale resolvable in the GPS phase data are of an order of tens of meters given the scan velocity of the GPS beam in the F_2 region and the 2 Hz sampling rate. Thus the experiment does not provide a direct proof that the observed GPS perturbations are caused by super small scale (SSS) irregularities such as predicted by *Gurevich and Zybin* [2006]. However, there are some indications that SSS irregularities play a role in this effect as discussed below.

[24] In fact, let us estimate the phase change due to GPS signals of frequency ω passing through the perturbed region of the ionosphere

$$\Delta\varphi = \frac{\omega}{c}\int \varepsilon dz \approx \frac{\omega}{c}\frac{\omega_e^2}{\omega^2}\frac{\delta n}{n} l \qquad (5)$$

where ε is the refraction index, $\omega_e = \sqrt{4\pi e^2 n/m}$ is the electron plasma frequency, δn is the electron density perturbations due to the HF-heating, and l is the length of the perturbed region. Consider the experiment 02/23/08 when the heating frequency was 4.3 MHz, and assume that $\omega_e \approx 2\pi \times 4.3 \times 10^6$ s^{-1} we obtain that

$$\frac{\delta n}{n} \approx \frac{10\ \Delta\varphi(\text{rad})}{l(\text{km})} \qquad (6)$$

Furthermore during the above experiment the observed differential phase was about 0.1 radians, while the width of the disturbed region does not exceed 5–10 km [*Gurevich*, 2007]. This gives the electron density perturbations of 10–20% which is almost an order of magnitude higher than that usually observed. Such enormous phase perturbations occurring on a one-second timescale indicate that scattering of GPS signals by the SSS irregularities could contribute to the differential phase observed.

[25] Beside the abrupt relaxation of STEC perturbations detected in our experiments (see the pulses marked by the arrows on Figure 2 (bottom)), shows that STEC relaxes to its unperturbed value within a fraction of a second after the termination of the HF pulse. The fast relaxation implies that it is caused by the ponderomotive force associated with the SSS irregularities, since the relaxation of the large scale irregularities occur on a much longer timescale [*Gurevich*, 2007]. Apparently no other process in the ionosphere can lead to such fast scattering of GPS signals.

[26] In conclusion, we presented the first experimental verification of the artificial perturbations of the diagnostic GPS signals. The results appear to be consistent with the presence of super small scale irregularities of the electron density caused by the HF-heating at the frequency close to 3 f_B, and offer important evidence in the support of the phenomena predicted by *Gurevich and Zybin* [2006]. Future analysis will be focused on measurements of intensity of the GPS signals rather than of its phases. If detected the perturbations of GPS intensity will be used as a diagnostic tool to describe the amplitude of SSS irregularities.

[27] **Acknowledgments.** The work was supported by the ONR Grant NAVY.N0017302C60 and by the ONR MURI Grant N000140710789. The experimental work was supported by the HAARP Program, Air Force Research Laboratory at Hanscom Air Force Base, Massachusetts, through the ONR contract N00014-02-C0463. We acknowledge Mike McCarrick, who helped in conducting the HAARP experiment, Lee Snyder, who supplied the ionospheric diagnostic data, Bill Bristow, who provided us with the radar data, and Thomas Leyser and Lars Norin, who provided us with the SEE data. We also appreciate helpful discussions with Dennis Papadopoulos.

References

Bakhmet'eva, N. V., et al. (1997), Investigation by backscatter radar of artificial irregularities produced in ionospheric plasma heating experiments, *J. Atmos. Sol. Terr. Phys.*, *59*, 2257.

Bishop, G. A., A. J. Mazzella Jr., and E. A. Holland (1995), Self-calibration of psuedorange errors by GPS two-frequency receivers, paper presented at 1995 National Technical Meeting, Inst. of Nav., Washington, D. C.

Dhillon, R., and T. R. Robinson (2005), Observations of time dependence and aspect sensitivity of regions of enhanced UHF backscatter associated with RF heating, *Ann. Geophys.*, *23*, 75.

Fialer, P. A. (1974), Field-aligned scattering from a heated region of the ionosphere: Observations at HF and VHF, *Radio Sci.*, *9*, 923.

Fremouw, E. J., R. L. Leadabrand, R. C. Livingston, M. D. Cousins, C. L. Rino, B. C. Fair, and R. A. Long (1978), Early results from the DNA Wideband satellite experiment: Complex-signal scintillation, *Radio Sci.*, *13*, 167.

Gondarenko, N. A., S. L. Ossakow, and G. M. Milikh (2005), Generation and evolution of density irregularities due to self-focusing in ionospheric modifications, *J. Geophys. Res.*, *110*, A09304, doi:10.1029/2005JA011142.

Gurevich, A. V. (2007), Nonlinear effects in the ionosphere, *Phys. Usp.*, *50*, 1091.

Gurevich, A. V., and K. P. Zybin (2006), Strong field aligned scattering of UHF radio waves in ionospheric modification, *Phys. Lett. A*, *358*, 159.

Gurevich, A. V., K. P. Zybin, and A. V. Lukyanov (1995), Stationary striations developed in the ionospheric modifications, *Phys. Rev. Lett.*, *75*, 2622.

Gurevich, A. V., A. V. Lukyanov, and K. P. Zybin (1996), Anomalous absorption of powerful radio waves on the striations developed during ionospheric modification, *Phys. Lett. A*, *211*, 363.

Hansen, J. D., G. J. Morales, L. M. Duncan, and G. Dimonte (1992), Large-Scale HF-Induced Ionospheric Modifications: Experiments, *J. Geophys. Res.*, *97*, 113.

Kelley, M. C., T. L. Arce, J. Salowey, M. Sulzer, W. T. Armstrong, M. Carter, and L. Duncan (1995), Density depletions at the 10-m scale induced by the arecibo heater, *J. Geophys. Res.*, *100*, 17,367.

Mjolhus, E. (1993), On the small scale striation effect in the ionospheric radio modification experiments near harmonics of the electron gyro frequency, *J. Atmos. Terr. Phys.*, *55*, 907.

Stubbe, P., A. J. Stocker, F. Honary, T. R. Robinson, and T. B. Jones (1994), Stimulated electromagnetic emissions and anomalous HF wave absorption near electron gyroharmonics, *J. Geophys. Res.*, *99*, 6233.

Thome, G. D., and D. W. Blood (1974), First observations of RF backscatter from field-aligned irregularities produced by ionospheric heating, *Radio Sci.*, *9*, 917.

Vaskov, V. V., and A. V. Gurevich (1976), Nonlinear resonant instability of a plasma in the field of ordinary electromagnetic wave, *Sov. Phys. JETP*, Engl., Transl., *42*, 91.

A. Gurevich and K. Zybin, P. N. Lebedev Institute, Russian Academy of Sciences, Moscow 117924, Russia.

G. Milikh, Department of Astronomy, University of Maryland, College Park, MD 20742-3921, USA. (milikh@astro.umd.edu)

J. Secan, Northwest Research Associates Inc., 2455 E. Speedway, 204, Tucson, AZ 85719, USA.